



Elucidation of structures of surface sulfate species on sulfated titania and mechanism of improved activity



Xuan Hao Lin^a, Xue Jiao Yin^a, Jun Yi Liu^a, Sam Fong Yau Li^{a,b,*}

^a Department of Chemistry, National University of Singapore, 3 Science Drive 3, Singapore 117543, Singapore

^b NUS Environmental Research Institute (NERI), #02-01, T-Lab Building (TL), 5A Engineering Drive 1, Singapore 117411, Singapore

ARTICLE INFO

Article history:

Received 18 August 2016

Received in revised form 17 October 2016

Accepted 24 October 2016

Available online 25 October 2016

Keywords:

Sulfated TiO₂

Superacid

Sulfate species

Brønsted acid

Lewis acid

ABSTRACT

Sulfated SO₄²⁻/TiO₂ superacid photocatalysts were synthesized and investigated for their photocatalytic activity and the structures of surface sulfate species. Six structures of sulfate species were elucidated using Fourier-Transform Infrared Spectroscopy. Correlation between the photocatalytic activity and structures of surface sulfate species were studied. The neutral Structures (IV) and (V) promoted the photocatalytic activity for the degradation of organic pollutants in reverse osmosis concentrate (ROC). Structure (II) was inactive. The acidic Structure (I) converted to (IV) when calcined at 600 °C or to (V) when neutralized. Brønsted acid amounts did not correlate to the photocatalytic activity while Lewis acid sites promoted the activity. Sulfated species-bonded Brønsted acid sites and Lewis acid sites and their transformation were observed with pyridine adsorption. Impact of surface area, crystal size and sulfate density on activity was also discussed. Mechanism of improved activity due to neutral sulfate species (IV) and (V) was also proposed. This study sheds some light on the mechanism of improved activity of sulfated photocatalysts and may also provide some clues to mechanism of other superacid catalysts.

© 2016 Elsevier B.V. All rights reserved.

1. Introduction

Reverse osmosis (RO) membrane technology has wide applications in wastewater recovery processes and desalination processes [1]. However, it also produces a certain quantity (15–25%) of reverse osmosis reject, i.e. reverse osmosis concentrate (ROC) [2]. ROC contains an increased amount of effluent organic matter (EfOM). Although EfOM is not considered to be a pollutant, it might be associated with undesirable organic compounds such as natural organic matter (NOM) and endocrine disruptors which limits reuse application. EfOM has been widely studies due to its promotion of membrane fouling [3]. Since ROC is not considered as a pollutant, currently ROC is usually discharged to water bodies, such as rivers, lakes, sea, and so on [4]. Many conventional methods (activated carbon, alum coagulation, air stripping) and advanced oxidation methods (AOPs) have been investigated to purify ROC, while results are still not satisfactory due to harmful by-products, low efficiency, high chemical cost or high capital investment cost [1,3–10]. Recently we reported high activity of internally sulfated TiO₂ photocatalysts for the degradation of organic pollutants in ROC

[11–13]. In this study, we further investigated the possible relationship between the photocatalytic activity and the structure of surface sulfate species.

Sulfation has been studied in many solid oxide catalysts, such as ZrO₂, Al₂O₃, SiO₂, Fe₂O₃ and TiO₂ [14–20]. It is known that sulfation creates Brønsted acid sites on the oxide surface. The ring-opening isomerization of cyclopropane is catalysed by Brønsted acids [21]. TiO₂/SO₄²⁻ was used as solid superacid photocatalyst for several substrates, such as ethylene, hexane, methanol, benzene, and trichloroethylene (TCE), etc. [22–25]. Sulfation may improve the catalytic activity from its increased Brønsted acid sites. Sulfation could be usually achieved by impregnating TiO₂ with 0.5 or 1.0 M H₂SO₄ or (NH₄)₂SO₄, or treating it with gases SO₂, SO₃ or H₂S and further oxidation with air or O₂ at elevated temperature [14,26]. After sulfation of ZrO₂ or TiO₂, surface Brønsted acid sites were increased which could be part of the reasons for the improved activity [27]. The electron withdrawing O=S=O groups at the surface of sulfated titania might function as electron traps [28]. Sulfation of TiO₂ extended its photocatalytic life and improved its thermal stability till 700 °C although no more SO₄²⁻ content at this temperature [27,29,30]. However, past reports on TiO₂/SO₄²⁻ mainly focused on activity, characterization and Brønsted acid amount but did not address the structures of surface sulfate species and the activity of individual sulfate species. In this study we report the structures of surface sulfate species, the activity of individual

* Corresponding author at: Department of Chemistry, National University of Singapore, 3 Science Drive 3, Singapore 117543, Singapore.

E-mail address: chmlifys@nus.edu.sg (S.F. Yau Li).

sulfate species, and the inter-conversion among different sulfate species.

2. Experimental

2.1. Materials

Titanyl sulfate (99.5%, AR), ethanol (95%, Reagent grade), absolute ethanol (99.9%, AR), Degussa P25 TiO₂, pyridine (99.9%, AR) and ammonia 25% (AR) were obtained from Sigma-Aldrich (St Louis, MO). Municipal ROC sample (5 l) was obtained from a Singapore water treatment plant and stored in fridge at 4 °C for all photocatalytic experiments here. Characteristics of the ROC samples were similar to those given in our previous work (see Supplemental Information) [12].

2.2. Preparation of sulfated titania

The sulfated titania photocatalysts were prepared through hydrolysis of TiOSO₄·xH₂O in ethanol/water solution. In a typical preparation, 4 g of titanyl sulfate was dissolved in 100 ml mixture of ethanol/water and hydrolysed for 6 h, followed by filtration and DI water rinsing. When the ethanol/water ratio was different, the dissolution time need for the 4 g of TiOSO₄·xH₂O was different. The slurry after rinsing was dried and calcined for 1 h. The synthesis conditions of 8 samples S1 to S8 are listed in Table 1.

2.3. Determination of Brønsted acid amount

The prepared sulfated titania photocatalysts were acidic. Their Brønsted acid amount were determined by titration with 0.05 M NaOH to pH value 7.0 ± 0.2 monitored with a pH meter. In a typical titration, 1.0 g of the catalyst was dispersed in 100 ml of DI water, then 0.05 M NaOH was dropped into the solution with stirring till pH value 6.8–7.2 while the pH value was monitored with a pH meter. After neutralization, the neutralized catalyst was filtered out and dried at 50 °C for overnight and named as S1N, S2N, S3N, S4N, S5N and S6N accordingly.

2.4. Characterization and photocatalytic reactions

The sulfated photocatalysts were characterized by X-ray diffraction (XRD) (Siemens D5005, Munich, Germany), N₂ sorption (Micromeritics ASAP 2020, Norcross, GA), scanning electron microscope (SEM) (JEOL JSM-6701F, Toyko, Japan), transmission electron microscope (TEM) (JEOL 3010, Toyko, Japan), energy dispersive spectroscope (EDS) (JEOL JSM-6701F, Toyko, Japan), UV-vis diffuse reflectance spectroscopy (UV-vis DRS) (Shimadzu 2450, Kyoto, Japan), Fourier transform infrared spectroscopy (FTIR) (IR Prestige 21 spectrometer, Shimadzu, Kyoto, Japan), X-ray photoelectron spectroscopy (XPS) (Omicron analyser EA125 7-channel spectrometer, Taunusstein, Germany), and photocatalytic reactions. Main characteristic properties of the sulfated titania are listed in Table 1. Photocatalytic reactions were conducted with 50 ml of ROC and 0.05 g of catalysts under monochromatic UV 365 nm irradiation (Mercury lamp, 100 W, 18 mW/cm², 6.467×10^{15} photons/s ml) for 6 h. Magnetic stirring was applied. Photocatalytic setup was shown in Fig. S1. Details of the photocatalytic setup, ROC sample analysis and catalyst characterization methods were reported in our previous work [11,12]. Before catalyst was added, the ROC sample had a pH value of 6.75. After catalyst was added, the ROC solution had a pH value range of 3.04–4.07 (Table S2, Supplementary data).

2.5. FTIR

FTIR samples were pre-treated at 110 °C for 8 h to get rid of adsorbed moisture. KBr was baked at 130 °C for 24 h. KBr pellet was pressed on a Shimadzu KBr pellet press equipped with a vacuum pump. The powder sample was vacuumed for 5 min and then pressed at 78.5 kn pressure with continuous vacuum for 15 min. Sample concentration in KBr powder was 0.5–1 %wt. Background spectrum was recorded on a pure KBr pellet in air at room temperature (25 °C) and was subtracted from the sample spectrum at the same temperature. The IR spectra were recorded by accumulating 32 scans at a spectral resolution of 4 cm⁻¹.

2.6. Pyridine adsorption

Pyridine adsorption experiments were conducted to probe the Brønsted and Lewis acid sites on the sulfated titania. A typical procedure was as below: a grinded powder sample (sulfated titania photocatalysts and KBr) was heated at 110 °C for 8 h and then transferred to a vacuum chamber (0.01 Torr or 1.33 Pa) for 16 h, pyridine adsorption was carried out at ambient temperature by allowing a large pyridine dose (10 Torr or 1333 Pa) over the vacuumed sample, and then evacuating at the same temperature to remove the excess pyridine after 30 min of adsorption. Finally the powder sample with adsorbed pyridine was pressed into a pellet as described in Section 2.5 for FTIR analysis.

3. Results

3.1. Photocatalytic activities of SO₄²⁻/TiO₂

3.1.1. Photocatalytic degradation of organics in ROC

The prepared SO₄²⁻/TiO₂ photocatalyst samples S1 to S8 were anatase phase with an average crystal size of 4–13 nm, band gap of 3.13–3.26 eV and S content of 1.38–15.76 %wt (Table 1). Four samples (S1, S2, S3 and S8) had higher photocatalytic activity than that of Degussa P25 for the degradation of organic pollutants (mainly natural organic matters (NOM), pharmaceuticals, surfactants, etc.) in ROC (Fig. 1a). However, the other 4 catalysts S4 to S7 were not as good as P25. Among these catalysts, S8 performed the best.

3.1.2. Impact of S content, pH value, crystal size and surface area

The photocatalytic performance was closely, although non-linearly, related to the sulfur content in the catalysts (Fig. 1b). The catalysts with less S contents had better performance while those with higher than 6% S content (i.e. S4, S5, S6, S7) had low photocatalytic activities.

pH values after catalysts were dispersed in the ROC samples could have some impact on the photocatalytic activities. As shown in Table S2, after sulfated catalysts (S1–S8) were added pH values of the ROC samples dropped from 6.75 to a range of 3.04–4.07. Based on our studies (unpublished data), at pH values of 2.5 and 10.6 degradation of Rhodamine B with TiO₂ were slightly faster than that at neutral pH of 6.3, and at pH 4.2 degradation rate of Rhodamine B with TiO₂ was very close to that at pH 6.3. Therefore, impact of the pH range of 3.04–4.07 on the photocatalytic activities of sulfated TiO₂ should be negligible. In addition, after catalyst neutralization activities of sulfated TiO₂ photocatalysts were improved, which also indicated little activity contribution from the lower pH range of 3.04–4.07.

Photocatalytic activities of the evaluated TiO₂ photocatalyst samples reached maximum with the crystal size of around 12 nm (Fig. 2a). Below 12 nm, the activities became lower due to higher chance of recombination of photogenerated electrons and holes. Above 12 nm, the activities also became lower due to the less photo-generated electrons and holes per crystal unit cell. However, there

Table 1

Catalysts, surface area, crystallographic phase, particle size, sulfur content and band gap.

Catalysts	W/E ratio ^a	Calc. temp. (°C) & time (hr)	S_{BET} (m ² /g)	Phase	PS ^b (nm)	S content (%wt.) ^c	E_g ^d (eV)
P25 ^e	/	/	49.8	Anatase & rutile	24 (A) 37 (R)	/	3.21
S1	100/0	400, 1	165.1	Anatase	6.06	3.34	3.25
S2	80/20	400, 1	146.9	Anatase	6.40	3.79	3.26
S3	67/33	400, 1	6.7	Anatase	6.30	4.79	3.21
S4	50/50	400, 1	17.8	Anatase	5.64	6.34	3.17
S5	33/67	400, 1	1.4	Anatase	5.04	8.25	3.13
S6	20/80	400, 1	2.9	Anatase	4.82	8.94	3.13
S7	0/100	400, 1	2.2	Anatase	/	15.76	3.20
S8	80/20	600, 1	69.7	Anatase	12.10	1.38	3.24

^a W/E ratio is the water/ethanol ratio in the hydrolysis solution during synthesis.

^b PS is the average particle size calculated from powder XRD data.

^c S content is the sulfur content determined by ICP/MS.

^d E_g is the indirect band gap determined from Tauc plots derived from solid UV-vis DRS data.

^e Degussa P25.

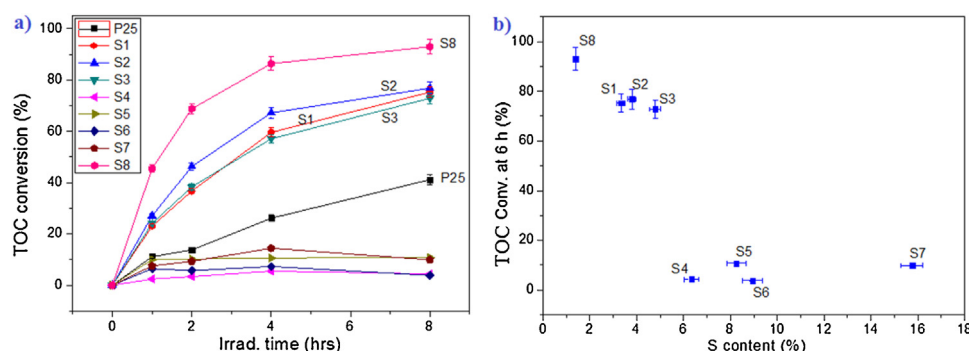


Fig. 1. a) Photocatalytic degradation of organic pollutants (Total organic content/carbon, TOC) in ROC with $\text{SO}_4^{2-}/\text{TiO}_2$ catalyst samples under monochromatic UV 365 nm irradiation (100W mercury lamp, 18 mW/cm², 6.467×10^{15} photons ml), b) Photocatalytic activities (irradiation for 6 h) of catalysts with different S contents.

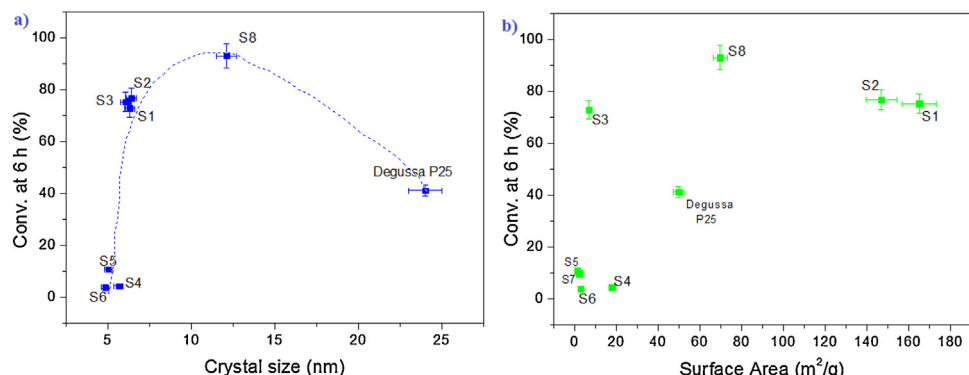


Fig. 2. Photocatalytic activities of catalyst samples with different (a) crystal sizes and (b) surface areas.

was no correlation between photocatalytic activities and surface area (Fig. 2b). Sample S3 had high activity even though its surface area was as low as 6.7 m²/g (measured twice). Sample S8 had the highest activity although it had only medium surface area of 69.7 m²/g. Sample S1 and S2 had much higher surface areas (165.1, 146.9 m²/g) than S8, but had significantly lower activities than S8. Although photoreactivity was usually regarded as a surface phenomenon and for many catalysts activity correlates well with surface area, in our case photocatalytic activity of sulfated TiO₂ did not correlate well with surface area. Hence, other factors might play more important roles in the photocatalytic activity of sulfated TiO₂. These activity-related factors could include crystal size, sulfate content, structure of different sulfate species, Brønsted acid sites, Lewis acid sites and so on.

3.1.3. Impact of Brønsted acid sites

As these catalysts were superacid, their Brønsted acid amounts were determined and the H⁺/Ti⁴⁺ mole ratios (atomic ratios) of the catalysts were calculated (Table 2). The Brønsted acid was from H₂SO₄ generated from hydrolysis of the precursor TiOSO₄. With less water in the water/ethanol mixture during synthesis, the precursor TiOSO₄ dissolution time was longer and the [H₂SO₄] after hydrolysis was also higher (Table 2) and therefore the Brønsted acid amount and S content in the final catalyst were higher. S1, S2 and S3 had medium Brønsted acid amounts while S4 had very high Brønsted acid amounts. S5, S6 and S8 had low Brønsted acid amounts. Fig. 3a shows that photocatalytic activity did not correlate well with Brønsted acid amounts per unit mass. S5, S6 and S8 had similar Brønsted acid amounts per mass, but S8 had much higher activity than those of S5 and S6. Since photocatalytic reac-

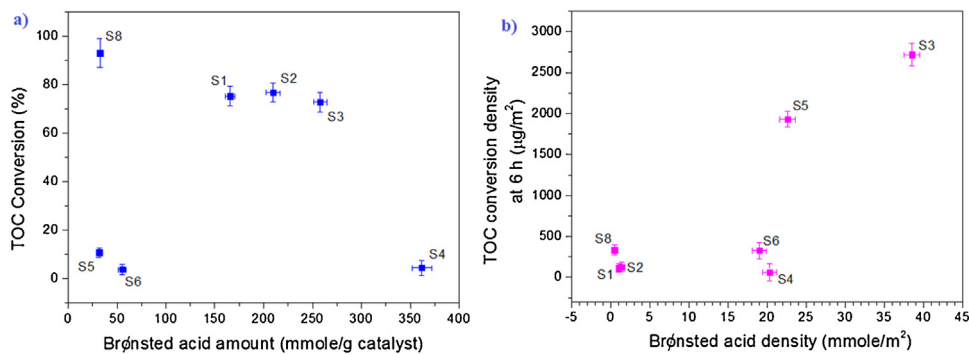


Fig. 3. a) Changes of TOC conversion with different Brønsted acid amounts on catalysts, b) Changes of TOC conversion density per unit surface area of catalysts with different Brønsted acid density per unit surface area of catalysts.

Table 2

Amount of Brønsted acid titrated by NaOH.

Catalysts	NaOH ^a (mmole/g cat.)	H ⁺ /Ti ⁴⁺ (%mole)	Time ^b (h)	[SO ₄ ²⁻] ^c (%wt.)
S1	165.7	13.24	1.0	1.83
S2	209.8	16.76	1.0	2.29
S3	257.9	20.60	2.5	2.73
S4	361.8	28.90	3.5	3.66
S5	31.7	2.53	6.0	5.55
S6	55.1	4.40	17.0	9.15
S7	/	/	ND ^d	/
S8	32.5	2.60	1.0	2.29

^a NaOH amount required for neutralization corresponds to Brønsted acid amount.

^b Dissolution time of precursor before hydrolysis.

^c Sulfate ion concentration in the hydrolysis solution during the catalyst preparation.

^d Not dissolved at all.

tions are surface phenomenon, activity could possibly be related to active sites at the surface which are limited by surface area. Therefore, we also calculated activities and Brønsted acid amounts per surface area and plotted them in Fig. 3b. Fig. 3b shows there could be some positive correlation between activity density and Brønsted acid density. However, the correlation was weak as there were outliers (i.e. S4 and S6). In order to further investigate this aspect, we neutralized the Brønsted acid sites of the sulfated catalysts by neutralizing their dispersions in DI water with NaOH solution to pH 7 and investigate the photocatalytic activity after catalyst neutralization. The results obtained are described in the Section 3.1.4.

3.1.4. Photocatalytic activities before and after catalyst neutralization

After the Brønsted acid sites were neutralized, photocatalytic activities of S1, S2, and S3 (S1N, S2N, S3N) were improved; the activity of S4 (S4N) was largely improved; while activities of S5 and S6 (S5N, S6N) were not improved (Tables 3 and 4). This indicates that photocatalytic activity could be only partially but not fully attributed to Brønsted acid sites. Fig. 4a and b shows activities of catalyst with different surface areas before and after neutralization. Activities of SO₄²⁻/TiO₂ catalysts did not correlate well with surface areas either before or after neutralization.

3.1.5. Photocatalytic activities and sulfate densities in the surface shell and bulk core of catalysts

Since photocatalytic reactions are surface phenomenon, the photocatalytic activity may be affected by the surface sulfate species. Therefore, besides the S content (%wt.) determined by ICP/MS we further examined the sulfate densities in the whole particles, surface shell and bulk core. With reference to our previous report [1], we determined the sulfate densities of surface shell and bulk core in S3 and S6 by XPS and ICP/MS. S6 had 6.34%wt. of S con-

tent, much higher than that of S3 (4.79%wt.). Table 5 shows that the bulk core sulfate density of S6 (1.623 nm⁻³) was higher than that of S3 (0.714 nm⁻³), while their surface sulfate densities were quite close, i.e. 2.87 nm⁻³ (S6) and 2.67 nm⁻³ (S3), respectively. Hence we assumed that for the other 6 sulfated photocatalysts their surface sulfate densities were also close. We used an average value of 2.77 nm⁻³ based on the values for S6 and S3 (Table 5). Table 5 shows that S1, S2, S3 and S8 had significantly lower sulfate densities in the bulk core and higher activities than those of S4, S5, S6 and S7. As mentioned in our previous report [1], sulfate groups are electron withdrawing groups and act as electron traps in sulfated TiO₂. The high sulfate densities in the bulk core could attract and trap electrons photogenerated from the surface, so that these photogenerated electrons could not be utilized for reactions but recombine with positive holes in the bulk core. Therefore, the high sulfate densities in the bulk core reduced photocatalytic activities. Sulfated TiO₂ catalysts with similar surface sulfate densities had very different photocatalytic activities, which indicated surface sulfate density did not correlate with photocatalytic activity. Nevertheless, improved photocatalytic activity after catalyst neutralization together with observed changes of FTIR spectra before and after neutralization hinted different types of sulfate species may explain such improved activity.

3.2. Structure of surface sulfate species

3.2.1. FTIR of various sulfur species

To facilitate interpretation of the IR peaks of the prepared SO₄²⁻/TiO₂ photocatalyst samples, a summary of various S species reported in the literature is given in the Supplementary information [31–40].

3.2.2. FTIR of sulfate species on SO₄²⁻/TiO₂

IR peaks of sulfate species on the SO₄²⁻/TiO₂ samples are mainly located at 1500–700 cm⁻¹ (Fig. 5). 1636 cm⁻¹ was the δH₂O band, i.e. H—O—H bending for H₂O molecule adsorbed on surface. S1, S2, S3 and S4 had the same 5 peaks at 1400, 1215, 1148, 1051 and 980 cm⁻¹. These 5 peaks are similar to but not exactly the same as the 5 peaks of the previously reported SO₃ adsorbed on TiO₂ at 1370, 1315, 1100, 1045 and 1005 cm⁻¹ which was assigned to (M—O)₂SO₂ or (M—O)₃S=O [26,39]. Considering high concentration of Brønsted acid amount ranging from 165.7 to 361.8 mmol/g catalyst on these four SO₄²⁻/TiO₂ samples (Table 2), we assigned these

Table 3

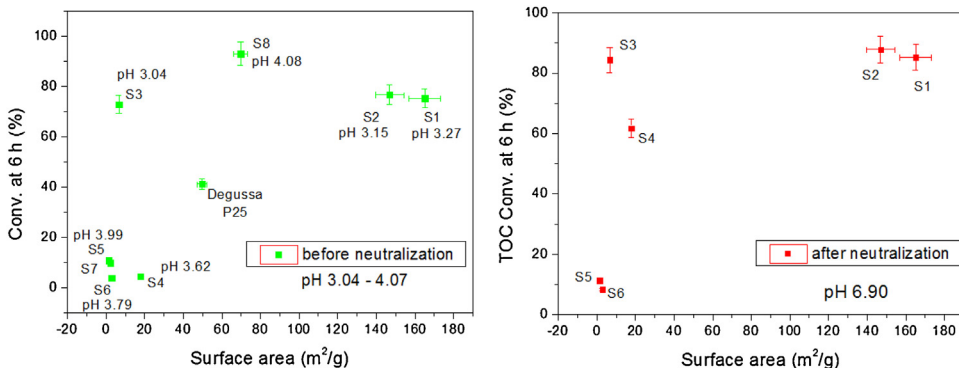
Photocatalytic activity before and after catalyst neutralization.

Catalysts	TOC Conv. (%)							
	Before neutralization				After neutralization			
	1 h	2 h	4 h	6 h	1 h	2 h	4 h	6 h
P25	11.1	13.8	26.1	41.2	/	/	/	/
S1	23.1	36.7	59.6	75.3	30.5	56.4	75.0	85.2
S2	27.1	46.3	67.2	76.8	36.3	64.9	79.0	87.8
S3	24.1	38.3	57.1	72.9	29.9	53.0	72.1	84.4
S4	2.4	3.4	5.5	4.4	14.2	27.6	44.8	61.7
S5	10.0	10.2	10.6	10.8	10.9	10.3	10.8	11.3
S6	6.5	5.7	7.3	3.8	6.6	5.9	8.3	8.3
S7	7.5	9.3	14.4	9.9	/	/	/	/
S8	45.5	68.8	86.4	93.0	/	/	/	/

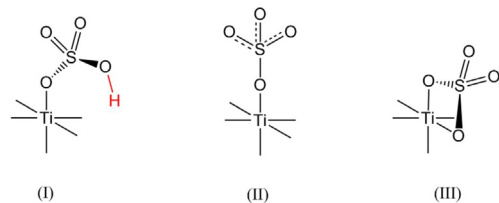
Table 4

Impact of Brønsted acid concentration and its surface density on TOC conversion efficiency.

Samples	S _{BET} (m ² /g)	Catalyst surface area per test (m ²) ^a	Brønsted acid concentration (mmole/g)	Surface Brønsted acid density (mmole/m ²) ^b	TOC Conv. At 6 h (%)	TOC qty converted in 6 h (μg) ^c	TOC Conversion density (μg/m ²) ^d	Activity of Brønsted acid sites (μg/mmole) ^e	(Before neutr.)	(After neutr.)	(Before neutr.)
									(Before neutr.)	(After neutr.)	(Before neutr.)
Degussa P25	49.8	1.494	/	/	41.2	/	309.0	206.8	/		
S1	165.1	4.953	165.7	1.00	75.3	85.2	564.8	114.0	113.6		
S2	146.9	4.407	209.8	1.43	76.8	87.8	576.0	130.7	91.5		
S3	6.7	0.201	257.9	38.49	72.9	84.4	546.8	2720.1	70.7		
S4	17.8	0.534	361.8	20.33	4.4	61.7	33.0	61.8	3.0		
S5	1.4	0.042	31.7	22.64	10.8	11.3	81.0	1928.6	85.2		
S6	2.9	0.087	55.1	19.00	3.8	8.3	28.5	327.6	17.2		
S7	2.2	0.066	/	/	9.9	/	74.3	1125.0	/		
S8	69.7	2.091	32.5	0.47	93	/	697.5	333.6	715.4		

^a Catalyst surface area per test (m²)=Surface area S_{BET} (m²/g) × 0.03 g of catalyst in 30 ml of ROC sample.^b Surface Brønsted acid density (mmole/m²)=Brønsted acid concentration (mmole/g)/Surface area S_{BET} (m²/g).^c TOC qty converted in 6 h (μg)=TOC Conv. At 6 h (%) × Initial ROC concentration × Volume of ROC sample.^d TOC conversion density (μg/m²)=TOC qty converted in 6 h (μg)/Catalyst surface area per test (m², per 0.03 g in 30 ml of ROC).^e Activity of Brønsted acid sites (μg/mmole)=TOC conversion density (μg/m²)/Surface Brønsted acid density (mmole/m²) assuming activity contributed solely from Brønsted acid sites.**Fig. 4.** Photocatalytic activities of SO₄²⁻/TiO₂ catalysts with different BET surface areas before and after neutralization of catalysts with NaOH.

5 IR peaks to the Structure (I). Peak at 1400 cm⁻¹ is a characteristic peak of the Structure (I).



S5 and S6 had 4 IR peaks at 1427, 1285, 1120 and 760 cm⁻¹. They could not hydrolyze further in water at room tempera-

ture. Due to the highest wavenumber peak at 1427 cm⁻¹ and low Brønsted acidity, these 4 peaks were assigned to the Structure (II) and attributed to the asymmetric and symmetric (1427, 1285 & 1120 cm⁻¹) stretching of S=O and the symmetric stretching of S-O. Peaks at 1427 and 760 cm⁻¹ are characteristic peaks of the Structure (II). S7 was prepared from 100% ethanol without water and it was not dissolved in ethanol. FTIR spectra showed that S7 was the same as the precursor TiOSO₄. In addition, S7 could still hydrolyze when water was added to it. Therefore, the 5 peaks of S7 at 1335, 1260, 1148, 998 and 820 cm⁻¹ were assigned to the Structure (III).

As shown in Fig. 6, besides sulfate peaks in the range of 800–1800 cm⁻¹ samples S1 to S8 had IR peaks at 3405 and

Table 5

Calculated sulfate densities in the surface shell and bulk core of catalysts.

Samples	S_{BET} (m^2/g)	S content by ICP/MS (%wt.)	Sulfate density in catalyst (nm^{-3})	Surface shell sulfate density (nm^{-3}) ^a	Bulk core sulfate density (nm^{-3}) ^b	TOC conv. At 6 h (%)
Degussa P25	49.8	0	/	/	/	41.2
S1	165.1	3.34	0.806	2.77 ^c	0.191	75.3
S2	146.9	3.79	0.914	2.77 ^c	0.344	76.8
S3	6.7	4.79	1.155	2.67	0.714	72.9
S4	17.8	6.34	1.529	2.77 ^c	1.029	4.4
S5	1.4	8.25	1.990	2.77 ^c	1.543	10.8
S6	2.9	8.94	2.156	2.87	1.623	3.8
S7	2.2	15.76	3.801	2.77 ^c	2.967	9.9
S8	69.7	1.38	0.333	2.77 ^c	0.058	93

^a Surface shell sulfate density (nm^{-3}) was determined by XPS and ICP/MS reported in our previous work [12]. Surface shell means the 7 nm thick outer surface layer of catalyst particles (aggregate of crystals), 7 nm is the average depth that XPS could penetrate.

^b Bulk core sulfate density (nm^{-3}) was determined by XPS and ICP/MS reported in our previous work [12].

^c This value (2.77) was based on an assumption that the surface sulfate density were very close which was observed from sample S3 and S6 with XPS. This value 2.77 was an average of those values of S3 and S6.

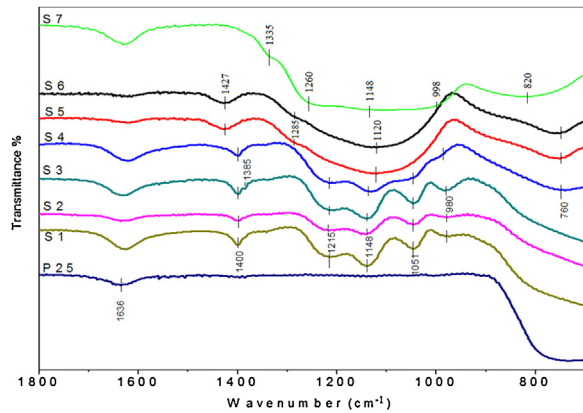


Fig. 5. FTIR spectra of $\text{SO}_4^{2-}/\text{TiO}_2$ photocatalyst samples S1–S7.

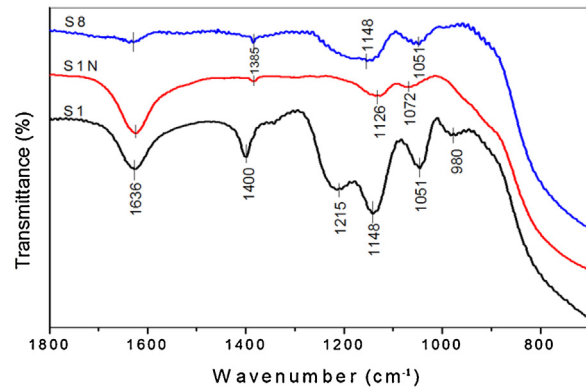


Fig. 7. IR spectra of S1, S1N (neutralized S1) and S8.

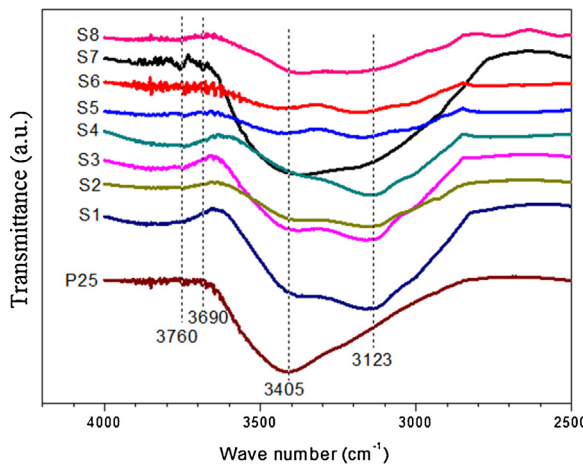


Fig. 6. FTIR spectra of samples at high wave number 4000–2500 cm^{-1} .

3123 cm^{-1} . Degussa P25 had one peak at 3405 cm^{-1} but no peak at 3123 cm^{-1} . The peak at 3405 cm^{-1} was assigned to moisture hydrogen bonded to Ti—, Ti—O—H and Ti—O, while the peak at 3123 cm^{-1} was assigned to moisture hydrogen bonded to sulfate species. Some weak peaks were shown in 3600–3800 cm^{-1} , which were reported to be mainly attributed to Ti—O—H. However there was no significant spectral difference in the range of 3600–3800 cm^{-1} among the samples except for slightly stronger peaks at 3760 and 3690 cm^{-1} for sample S7, which could be due to its hydrolysis with adsorbed moisture since its hydrolysis solution was pure ethanol without

water. Low activity of S7 indicated that Ti—O—H might not have catalytic activity alone by itself.

3.3. Effect of different sulfate species on photocatalytic activity

The difference of the synthesis conditions between the S1 and S8 was the calcination temperature, S1 was calcined at 400 °C for 1 h while S8 was calcined at 600 °C for 1 h (Table 1). S1 had high Brønsted acid amount corresponding to 165.7 mmol/g catalyst while S8 had 5 times lower Brønsted acid amount corresponding to 32.5 mmole/g catalyst. S1 had 5 sulfate related IR peaks at 1400, 1215, 1148, 1051 and 980 cm^{-1} . But S8 had only 3 sulfate related IR peaks at 1385, 1148 and 1051 cm^{-1} (Fig. 7). Fewer IR peaks of S8 implied higher symmetry of its sulfate species. The disappearance of the characteristic peak of the acidic Structure (I) at 1400 cm^{-1} on S8 indicated that S8 did not have the Structure (I). From the 5 times lower Brønsted acid amount and higher symmetry of sulfate species of S8 compared with S1, it was possible that the acidic Structure (I) in S1 already converted to the neutral Structure (IV) in S8 with higher calcination temperature. According to our previously reported XPS data, the Structures (IV-a), (IV-b) and (IV-c) may also exist on S8 (Fig. 8) [12]. S8 had higher photocatalytic activity for the degradation of organic pollutants in ROC than S1. The better

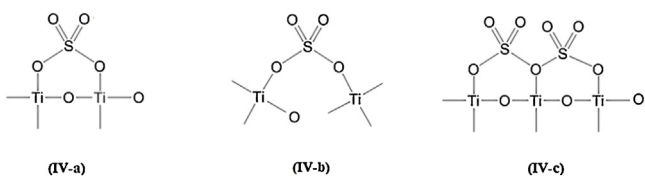


Fig. 8. Structures (IV-a), (IV-b) and (IV-c). For simplification, only 4 bonds on Ti were drawn.

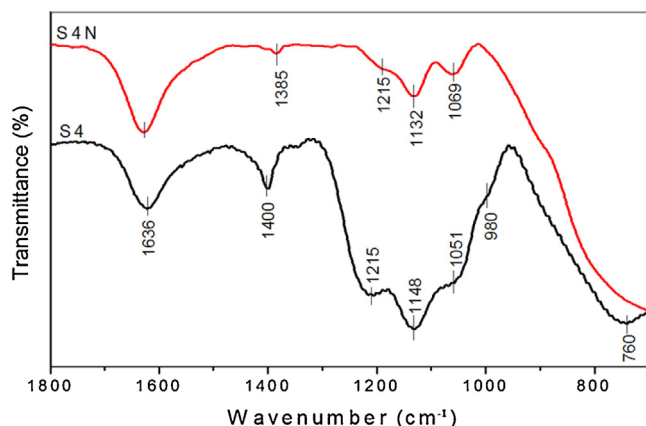
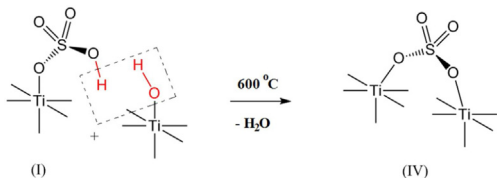
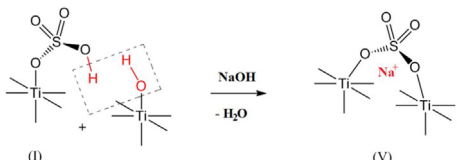


Fig. 9. FTIR spectra of S4 and S4N (after neutralization).

activity of S8 than that of S1 could be attributed to crystal size, bulk core sulfate density, and different types of surface sulfate species.

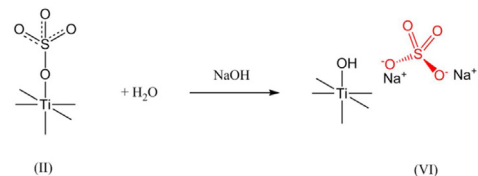


S1 had 5 sulfate related IR peaks at 1400, 1215, 1148, 1051 and 980 cm⁻¹. After S1 was neutralized, the S1N (neutralized S1) only had 3 sulfate related IR peaks at 1385, 1126 and 1072 cm⁻¹ (Fig. 7), which were very similar and close to the 3 peaks of S8 at 1385, 1148 and 1051 cm⁻¹. So the structure of sulfate species in S1N and S8 could be very similar. According to the neutralization of the acidic Structure (I) and the similarity to the Structure (IV), Structure (V) was assigned to the sulfate species of S1N. Since species (V)-riched S1N was more efficient in the photocatalytic degradation of organic pollutants in ROC than species (I)-riched S1, Structure of (V) should be also more photocatalytically active than Structure (I). Activity of Structure of (IV) should be close to that of Structure (V) due to their structure similarity.

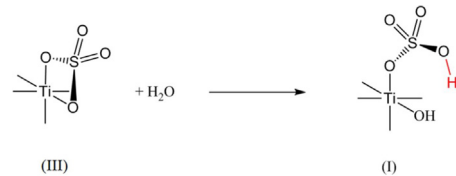


Because S5 and S6 performed relatively poorly in the photocatalytic degradation of organic pollutants in ROC, Structure (II) should have much lower photocatalytic activity than Structure (I). S4 also had a peak at 760 cm⁻¹, which was characteristic of Structure (II) (Fig. 9). Hence, S4 may also contain small amount of Structure (II), besides the main Structure (I). After neutralization the S4N (neutralized S4) did not have the peak at 760 cm⁻¹ anymore, which indicated that Structure (II) disappeared (likely hydrolyzed) dur-

ing neutralization. Based on the results from samples S5 and S6 we understood that Structure (II) was difficult to hydrolyze. The possible reasons for the hydrolysis of a small amount of Structure (II) in S4 could include co-existence of the acidic Structure (I) and relatively small amount of Structure (II). Compared with S1N, S4N had an additional peak at 1215 cm⁻¹, which could be attributed to inorganic sulfate ions. Therefore, during neutralization, the small amount of Structure (II) in S4 may hydrolyze and be neutralized to form Structure (VI), i.e. inorganic sulfate ions. Inorganic sulfate ions might not improve the photocatalytic activities, but the improved activity of S4N over S4 could be attributed to newly generated surface Ti—OH groups.



The Structure (III) in S7 was the same as that in the precursor TiOSO₄ and could further hydrolyze. When its hydrolysis conditions were the same as those for S1, S2, or S3 Structure (III) converted to Structure (I).



3.4. Sulfate species-bonded Brønsted acid sites and Lewis acid sites

The different types of samples after adsorbing pyridine were named as sample-Py, such as S1-Py, S1N-Py, S2-Py, S2N-Py, etc (Fig. 10). After pyridine adsorption, samples S1 and S1N (S1-Py and S1N-Py) showed peaks at 1489, 1506 and 1540 cm⁻¹ attributed from Brønsted acid sites (Fig. S1) [27,39,41–43]. They also showed peaks at 1456, 1489 and 1506 cm⁻¹ attributed from Lewis acid sites. Other samples had higher noise level in 1420–1700 cm⁻¹ region which made it difficult to assign their Brønsted acid sites and Lewis acid sites. After pyridine adsorption, samples S1 to S4 had one additional peak at 1385 cm⁻¹ and the peaks at 1148 and 1051 cm⁻¹ were relatively more intense (Fig. 10). These 3 peaks were similar to those of Structure (IV). This indicated a partial conversion of Structure (I) to Structure (IV) after pyridine adsorption. Such conversion could indicate sulfate species-bonded Brønsted acid sites. S5 and S6 also showed a new peak at 1385 cm⁻¹ but the changes at 1148 and 1051 cm⁻¹ were not obvious, which could be due to much less amounts of sulfate species-bonded Brønsted acid sites on S5 and S6.

After pyridine adsorption onto the neutralized samples S1N, S2N, S3N and S4N, the peak at 1385 cm⁻¹ disappeared and two new peaks at 1400 and 1260 cm⁻¹ appeared (Fig. 10). The disappearance of the peak at 1385 cm⁻¹ indicated conversion of Structure (IV) to a new structure. Since the peak at 1400 cm⁻¹ was the characteristic peak of the acidic Structure (I), the new structure may contain sulfate species-related Brønsted acid sites. Since S1N, S2N, S3N and S4N were neutralized samples, and the peak at 1260 cm⁻¹ was different from the 5 peaks of the acidic Structure (I), the peak could be attributed to the sulfate species on Lewis acid sites. The new structure after pyridine adsorption on neutralized samples was assigned to the Structure (IV-d). Structure (IV-d) could be derived from Struc-

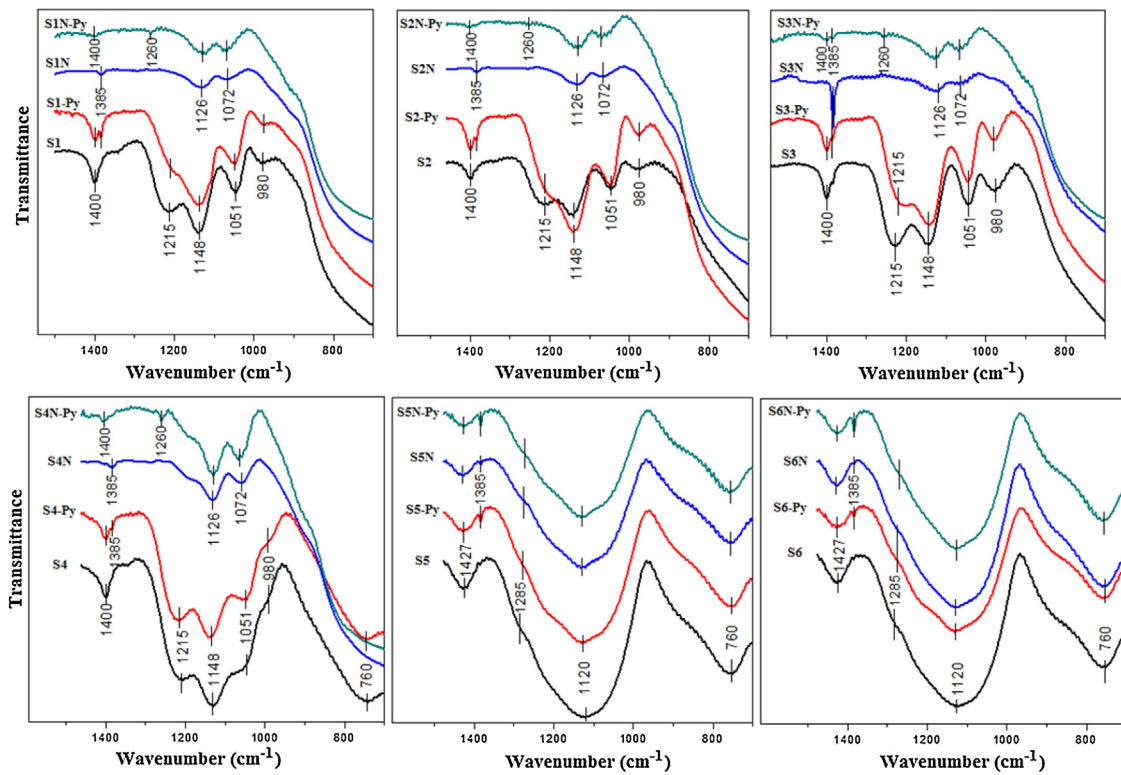
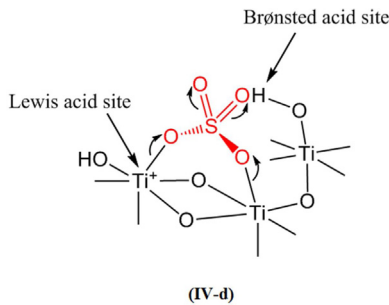


Fig. 10. FTIR spectra of S1-S6, after pyridine adsorption (-Py), after neutralization (N), and after both neutralization and pyridine adsorption (N-Py).

ture (IV) by the adsorption of pyridine [27,39,41–43]. In Structure (IV-d), pyridine could be adsorbed onto the Ti(IV) site bonded with a sulfate group, which then grabbed a proton from near-by Ti-OH re-generating a sulfate species-bonded Brønsted acid site. Pyridine adsorbed on the sulfate species-bonded Lewis acid site of the Structure (IV-d) could affect the vibration frequency of the sulfate species on the same Lewis acid site resulting in appearance of the peak at 1260 cm⁻¹. S5N and S6N did not have the peak at 1260 cm⁻¹ implying that they did not have sulfate species-bonded Lewis acid sites, which probably was one of the reasons for their low photocatalytic activity.



3.5. Mechanism of enhanced photocatalytic activity by surface sulfate species

In Section 3.3, we concluded that neutral sulfate species (IV) and (V) had higher activities than other sulfate species such as (I). Due to the structural similarity of (IV) and (V), to simply descriptions here we compare only (IV) and (I). Molecular orbitals of pure anatase TiO₂ are composed of orbitals of Ti⁴⁺ and O²⁻ ions. Each Ti⁴⁺ ion is surrounded by 6 O²⁻ ions while each O²⁻ ion is surrounded by 3 Ti⁴⁺ ions. σ and σ^* orbitals were formed by the orbital 2p_z of O²⁻ ion and the 3d_{z²} (one of the two 3e_g orbitals) and 4s of Ti⁴⁺

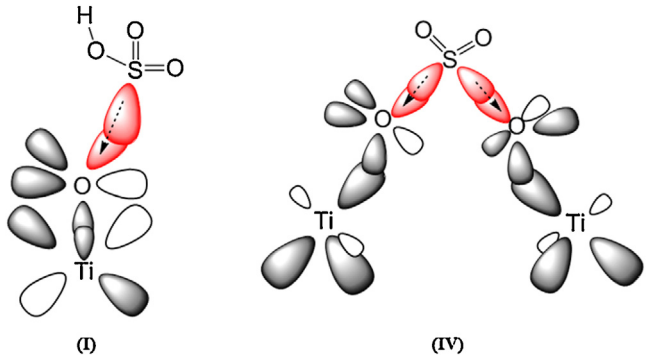


Fig. 11. Mechanism of enhanced photocatalytic activity by surface sulfate species (IV) on SO₄²⁻/TiO₂ photocatalysts.

ion [44–46]. The orbitals 2p_x and 2p_y of O²⁻ ion and the 3d_{xz} & 3d_{yz}, i.e. two of the three 3t_{2g} orbitals, and 4p orbitals of Ti⁴⁺ ion formed π and π^* orbitals. Titanium dioxide is partially covalent and partially ionic, resulting in an insulating stoichiometric crystals. In stoichiometric TiO₂, theoretically Ti⁴⁺ and O²⁻ form bonds through one σ and one π bonds. To simply the orbital drawing, orbitals 4s and 4p of Ti⁴⁺ ion were not drawn in Fig. 11. O²⁻ of species (I) fed both σ and π electron cloud into Ti 3d_{z²} and 3d_{xz} (or 3d_{yz}) orbitals. O²⁻ of species (IV) fed only σ electron cloud into Ti⁴⁺ 3d_{z²} without feeding any π electron cloud, forming one σ bond but no π bond due to bond angle constrain from orientation mismatch. Fig. 11 shows that sulfate species (I) was indirectly bonded to one Ti⁴⁺ only while sulfate species (IV) was indirectly bonded to two Ti⁴⁺. Ti⁴⁺ is electron deficient and withdrawing. Indirect bonding to two Ti⁴⁺ through O²⁻ made S⁶⁺ in species (IV) more electron deficient and electron withdrawing than that in species (I), resulting in species (IV) having a deeper electron trap than species (I). Deeper electron

trapping effect from species (IV) enabled them to induce better e⁻-h⁺ separation and hence better photocatalytic activity.

4. Conclusions

Six sulfate species on sulfated SO₄²⁻/TiO₂ superacid photocatalysts were elucidated according to their FTIR spectra and other properties. For the active SO₄²⁻/TiO₂ photocatalysts, their photocatalytic activities for the degradation of organic pollutants in ROC did not correlate to their surface areas and Brønsted acid amounts. Instead, activities could be more attributed to crystal size, sulfate densities in bulk core and types of surface sulfate species. When neutralized, these photocatalysts showed higher efficiency. Activity sequence of the surface sulfate species was as below: Structure (IV) ≡ (V) > (I) > (II) ≡ (III) > (VI). The acidic Structure (I) could convert to the neutral Structure (IV) at high temperature (600 °C) or convert to the sodium-adducted Structure (V) when neutralized. Structure (II) was inactive and difficult to hydrolyze, but at a small amount and together with Structure (I) it could hydrolyze and be neutralized to the inorganic Structure (VI). Structure (III) could easily hydrolyze to Structure (I) in water. Sulfate species-bonded Brønsted acid sites, i.e. Structure (I) and sulfate species-bonded Lewis acid sites, i.e. Structure (IV) were also observed by pyridine adsorption. With pyridine adsorption sulfate species-bonded Brønsted acid sites could be transformed from sulfate species-bonded Lewis acid sites through Structure (IV-d), i.e. a transition state. Higher activity of neutral sulfate species (IV) and (V) could be explained by their indirect bonding to two electron-deficient Ti⁴⁺ resulting in their S⁶⁺ more electron-withdrawing and both species themselves having deeper electron traps. While lower activity of species (I) only indirectly bonded to one electron-deficient Ti⁴⁺, resulting in (I) having a less deep electron trap.

Acknowledgements

We acknowledge the financial support from the National University of Singapore, National Research Foundation and Economic Development Board (SPORE, COY-15-EWI-RCFSA/N197-1), and Ministry of Education (R-143-000-582-112). We thank the Shenzhen Development and Reform Commission (SZ DRC) for supporting our collaborative project with Peking University Shenzhen Graduate School.

Appendix A. Supplementary data

Supplementary data associated with this article can be found, in the online version, at <http://dx.doi.org/10.1016/j.apcatb.2016.10.068>.

References

- [1] E. Dialynas, D. Mantzavinos, E. Diamadopoulos, Water Res. 42 (2008) 4603–4608.
- [2] K. Liu, F.A. Roddick, L.H. Fan, Water Res. 46 (2012) 3229–3239.
- [3] P. Westerhoff, H. Moon, D. Minakata, J. Crittenden, Water Res. 43 (2009) 3992–3998.
- [4] A. Perez-Gonzalez, A.M. Urtiaga, R. Ibanez, I. Ortiz, Water Res. 46 (2012) 267–283.
- [5] A.Y. Bagastyo, J. Radjenovic, Y. Mu, R.A. Rozendal, D.J. Batstone, K. Rabaey, Water Res. 45 (2011) 4951–4959.
- [6] J. Benner, E. Salhi, T. Ternes, U. von Gunten, Water Res. 42 (2008) 3003–3012.
- [7] D. Hermosilla, N. Merayo, R. Ordóñez, A. Blanco, Waste Manage. 32 (2012) 1236–1243.
- [8] A.Y. Bagastyo, J. Keller, Y. Poussade, D.J. Batstone, Water Res. 45 (2011) 2415–2427.
- [9] T. Zhou, T.T. Lim, S.S. Chin, A.G. Fane, Chem. Eng. J. 166 (2011) 932–939.
- [10] M. Lu, L. Guo, S. Kharkwal, H.N. Wu, H.Y. Ng, S.F.Y. Li, J. Power Sources 221 (2013) 381–386.
- [11] X.H. Lin, S.F.Y. Li, Desalination 344 (2014) 206–211.
- [12] X.H. Lin, S.F.Y. Li, Appl. Catal. B-Environ. 170–171 (2015) 263–272.
- [13] X.H. Lin, D. Sriramulu, S.F.Y. Li, Water Res. 68 (2015) 831–838.
- [14] F. Su, Y.H. Guo, Green Chem. 16 (2014) 2934–2957.
- [15] C. Contescu, V.T. Popa, J.B. Miller, E.I. Ko, J.A. Schwarz, Chem. Eng. J. 64 (1996) 265–272.
- [16] X.M. Song, A. Sayari, Catal. Rev. Sci. Eng. 38 (1996) 329–412.
- [17] T.S. Yang, T.H. Chang, C.T. Yeh, J. Mol. Catal. A-Chem. 123 (1997) 163–169.
- [18] A.S.C. Brown, J.S.J. Hargreaves, B. Rijniersce, Top. Catal. 11 (2000) 181–184.
- [19] G. Magnacca, G. Cerrato, C. Morterra, M. Signoretto, F. Somma, F. Pinna, Chem. Mat. 15 (2003) 675–687.
- [20] T. Rostovshchikova, V. Smirnov, O. Kiseleva, V. Yushchenko, M. Tzodikov, Y. Maksimov, I. Suzdalev, L. Kustov, O. Tkachenko, Catal. Today 152 (2010) 48–53.
- [21] A. Kayo, T. Yamaguchi, K. Tanabe, J. Catal. 83 (1983) 99–106.
- [22] Y.R. Ma, T.S. Jin, Z.H. Wang, T.S. Li, Indian J. Chem. Sect. B-Org. Chem. Incl. Med. Chem. 42 (2003) 1777–1778.
- [23] W.Y. Su, Y.L. Chen, X.Z. Fu, K.M. Wei, Chem. J. Chin. Univ.-Chin. 23 (2002) 1398–1400.
- [24] S. Yamazaki, N. Fujinaga, K. Araki, Appl. Catal. A-Gen. 210 (2001) 97–102.
- [25] H.L. Yin, Z.Y. Tan, Y.T. Liao, Y.J. Feng, J. Environ. Radioact. 87 (2006) 227–235.
- [26] O. Saur, M. Bensitel, A.B.M. Saad, J.C. Lavallee, C.P. Tripp, B.A. Morrow, J. Catal. 99 (1986) 104–110.
- [27] L.K. Noda, R.M. de Almeida, N.S. Goncalves, L.F.D. Probst, O. Sala, Catal. Today 85 (2003) 69–74.
- [28] R. Gomez, T. Lopez, E. Ortíz-Islas, J. Navarrete, E. Sanchez, F. Tzompantzis, X. Bokhimi, J. Mol. Catal. A-Chem. 193 (2003) 217–226.
- [29] X.Y. Deng, Y.H. Yue, Z. Gao, Appl. Catal. B-Environ. 39 (2002) 135–147.
- [30] D.S. Muggli, L.F. Ding, Appl. Catal. B-Environ. 32 (2001) 181–194.
- [31] J.P. Dunn, P.R. Koppula, H.G. Stenger, I.E. Wachs, Appl. Catal. B-Environ. 19 (1998) 103–117.
- [32] K. Nakamoto, Wiley: New York (1970).
- [33] G. Newman, D.B. Powell, Spectrochim. Acta (1963) 213.
- [34] M.E. Baldwin, J. Chem. Soc. (1961) 3123.
- [35] R.J. Gillespie, E.A. Robinson, Can. J. Chem. (1962) 644.
- [36] N.B. Colthup, J. Opt. Soc. Am. (1950) 644.
- [37] R.A. Marcus, J.M. Fresco, J. Chem. Phys. (1957) 564.
- [38] T. Yamaguchi, T. Jin, K. Tanabe, J. Phys. Chem. 90 (1986) 3148–3152.
- [39] C. Morterra, G. Cerrato, Phys. Chem. Chem. Phys. 1 (1999) 2825–2831.
- [40] J. Preud'homme, J. Lamotte, A. Janin, J.C. Lavallee, Bull. Soc. Chim. Fr. (1981) 433.
- [41] R. Srinivasan, R.A. Keogh, D.R. Milburn, B.H. Davis, J. Catal. 153 (1995) 123–130.
- [42] V. Parvulescu, S. Coman, P. Grange, V.I. Parvulescu, Appl. Catal. A-Gen. 176 (1999) 27–43.
- [43] K.J.A. Raj, M.G. Prakash, B. Viswanathan, Catal. Sci. Technol. 1 (2011) 1182–1188.
- [44] S. Agrawal, N.J. English, K.R. Thampi, J.M.D. MacElroy, Phys. Chem. Chem. Phys. 14 (2012) 12044–12056.
- [45] M.T. Greiner, Z.H. Lu, Npg Asia Materials 5 (2013).
- [46] H.L. Wang, T.C. Steinle, C. Apetrei, J.P. Maier, Phys. Chem. Chem. Phys. 11 (2009) 2649–2656.